

# 1

## Methane

### 1.1 Application

Methane is a simple gaseous hydrocarbon with the formula  $\text{CH}_4$  and a molecular weight of 16 g/mol. It is the main ingredient of natural gas which is defined as “dry gas” with a methane content of >80% and “wet gas” with a methane content of <80% (Thinkstep 2017). Natural gas also consists of ethane, propane, and butane referred to as the “natural gas liquids” (NGLs), which condense at lower temperatures and can rather easily be removed from natural gas. The NGLs may be channeled into diverse value chains for producing other chemicals like a cracking process in the ethane cracker to derive, e.g. ethylene and propylene, a dehydrogenation of propane to derive propylene, or a chemical conversion to C4 molecules with higher molecular functionality derived from butane.

Natural gas is mainly used as an energy source to generate heat and power or as a feedstock in the chemical industry like in the synthesis of acetylene, syngas, carbon monoxide, and methanol (Arpe 2007). Its global consumption is estimated about 3.800 bn  $\text{m}^3$  in 2020 (Focus 2021). The carbon footprint (scope 3) of methane varies between 6 and 30 g  $\text{CO}_2\text{e}/\text{MJ}$  (lower heating value [LHV]), depending on the specific extraction efforts and the distance between source and sink (OCI 2021; Gan et al. 2020; Thinkstep 2017). Natural gas is usually sold according to its energy content, and the price level is about 5–6 €/mmBTU in Europe and 2–3 €/mmBTU in the United States (OCI 2021; Focus 2021; Centi 2020; Capital 2019).

### 1.2 Conventional Production of Methane

Natural gas and methane, accordingly, are mainly produced via the exploitation of natural reservoirs. The process does not include a chemical conversion since methane is the main component of the gas mixture extracted out of the natural reservoir through some purification steps that comply with the specification of the respective grid. The local gas supplier is usually slightly adjusting the composition of natural gas to comply with the natural Wobbe index (Thema et al. 2019) and to ensure a rather constant heating value despite fluctuations and varying composition in the natural reservoir. For both the application of natural gas as fuel and chemical feedstock, it has been managed to use the gas mixture without costly processing efforts. The use of natural gas for the production of ammonia or syngas

for hydroformylations does usually not require isolating methane, though the natural gas mixture is channeled into the process.

Given the low extraction costs, alternative technologies for methane were traditionally not focused on. The rising interest in academia and the chemical and power industry for synthetic natural gas (SNG) or fermentative methane with carbon dioxide as feed is driven by sustainability considerations. Both technologies would presumably result in higher production costs, though might provide a huge leverage for the chemical use of carbon dioxide as a chemical building block. This shall be accomplished via the generation of green power based on photovoltaic cells and wind energy to provide green hydrogen via electrolysis, which would then be applied for the hydrogenation of carbon dioxide. The thermic use of methane or SNG would still generate carbon dioxide, though the net balance would be zero since each burnt mol of methane has beforehand consumed 1 mol of carbon dioxide.

Furthermore, methane shall be developed as energy storage (“power-to-gas,” Götz et al. 2016; Ewald et al. 2015). The shift to renewable production of energy derived from solar power and wind energy – which are not permanently available pending on daytime and season – combined with the prospected phasing out of fossil energy sources will require the development and installation of energy storage technology. Since conventional batteries are not economic for high power capacity, the chemical energy carriers hydrogen, ammonia, methanol, and methane are discussed (Rivard et al. 2019; Burkart et al. 2019; Spurgeon and Kumar 2018; Goepfert et al. 2014). All would have different advantages and disadvantages as energy storage if the criteria production cost, energy density, cost of transportation, and cost of storage and handling security are compared. The great advantage of methane would be that it can easily be stored and transported via the existing national gas grids. The German gas grid has a maximum capacity of 24.6 bn m<sup>3</sup> corresponding to an energy storage potential of about 246 TWh (Handelsblatt 2022; Güssgen et al. 2021; Ewald et al. 2015). This is a major advantage for methane as opposed to hydrogen for which – with some exceptions – a new transportation infrastructure would need to be installed. It is also considered to transport hydrogen in the existing gas grids and to selectively extract hydrogen at defined exit points. The current national grid regulations define a maximum hydrogen content of 0.1 up to 10% (v/v), and it needs to be ensured that the current equipment and material are suitable for hydrogen transportation with respect to potential attack of pipe material and diffusion loss (Rusmanis et al. n.d.). Accordingly, the chemical hydrogenation of carbon dioxide and the fermentative generation of methane with “green” hydrogen as energy source (Thema et al. 2019) have attracted attention.

### 1.3 Carbon Dioxide as Feedstock

The hydrogenation of carbon dioxide with green hydrogen may consume carbon dioxide from different feedstocks. In particular, the carbon dioxide might be captured at a power plant generating electrical power based on fossil fuels (e.g. the burning of natural gas or coal), at chemical plants that use natural gas as energy source (e.g. ammonia and hydrogen production), maybe captured out of the atmosphere via direct air capture (DAC; Ozkan et al. 2022; House et al. 2011), or be obtained in the upgrading of biogas. The fermentative production of biogas defines a technology field on its own. It applies various agricultural

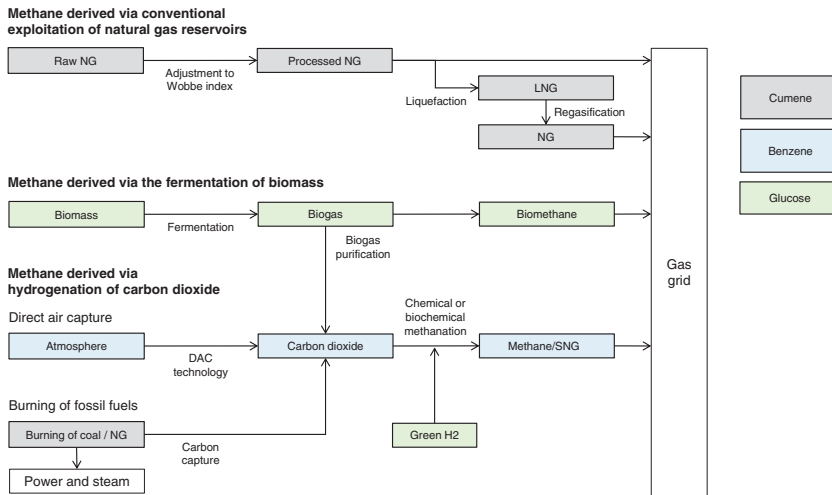


**Figure 1.1** Potential role of biological methanation in the generation of methane. Source: Walter Koch.

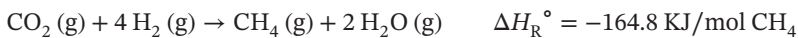
and organic feedstocks that, when digested by anaerobic bacteria, convert into basically 50–60% (v/v) methane and up to 35% (v/v) carbon dioxide. A broad mixture of hosts or microbial consortia, respectively, is used which are rather complex and characterized by diverse metabolic interactions. After the hydrolysis of the biomass, acidogenesis takes place. The generated organic fatty acids are then further digested by other fermenting bacteria into either acetic acid or carbon dioxide and hydrogen. Finally, methane formation proceeds via acetotrophic methanogenesis (acetate as substrate) and hydrogenotrophic methanogenesis (carbon dioxide and hydrogen as feedstock). The nonindustrial biogas technology is operated in a high number of local small-scale plants, mainly according to the local availability of agricultural waste streams. The obtained biogas is either directly burnt to generate heat or purified to biomethane and channeled into the gas grid (Adnan et al. 2019). Feeding the biomethane share of biogas into the gas grid requires the removal of carbon dioxide and would cause a rather high emission of carbon dioxide. In case hydrogen would be available, the carbon dioxide might be converted into additional methane and the emission of carbon dioxide would be avoided. Accordingly, the hydrogenation of carbon dioxide might also be applied for upgrading the quality of biogas to raise the methane output and avoid the emission of the by-product carbon dioxide. The technological options for the generation of methane, the sources of carbon dioxide, and the potential role of biological methanation may be summarized as follows (Figure 1.1).

Since a commercially reasonable hydrogen supply of the small and often nonindustrial biogas plants is difficult, specific boundary conditions for technology design are to be obeyed. The local generation of hydrogen would avoid high efforts for hydrogen processing and transportation. The direct integration of water electrolysis and hydrogenation of carbon dioxide with in situ conversion of hydrogen at the cathode might avoid the implementation of Environmental, Health and Safety (EHS) efforts to address the explosion risk in hydrogen handling, which might hamper commercial feasibility of local settings (Mayer et al. 2017).

## 1.4 Conversion of Carbon Dioxide into Methane

### 1.4.1 The Chemical Sabatier

The target reaction for the conversion of carbon dioxide into methane would be the direct reduction with molecular hydrogen. This reaction is sometimes referred to as the “chemical Sabatier” in honor of the historical discovery by P. Sabatier and J.-B. Senderens. Both are known for their pioneering work on catalytic hydrogenation originally with Nickel powder and were awarded with the Nobel Prize in 1912. The chemical and biotechnological conversion obtain water in different states of aggregation. The chemical hydrogenation is pursued at temperatures  $>100^\circ\text{C}$  and obtains water as steam:



The enthalpy of the reaction is estimated according to Hess’s law (Thema et al. 2019):

$$\begin{aligned} \Delta H_{\text{R}}^\circ &= \Sigma \Delta H_{\text{f}}^\circ_{\text{P}} - \Sigma \Delta H_{\text{f}}^\circ_{\text{E}} = (-74.8 \text{ KJ/mol} + 2 \times -241.8 \text{ KJ/mol}) - 393.3 \text{ KJ/mol} \\ &= -164.8 \text{ KJ/mol given} \end{aligned}$$

$$\Delta H_{\text{f}}^\circ \text{CO}_2(\text{g}) = -393.3 \text{ KJ/mol,}$$

$$\Delta H_{\text{f}}^\circ \text{CH}_4(\text{g}) = -74.8 \text{ KJ/mol and}$$

$$\Delta H_{\text{f}}^\circ \text{H}_2\text{O}(\text{g}) = -241.8 \text{ KJ/mol}$$

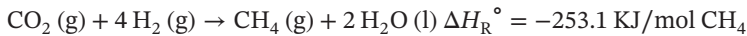
The maximum stoichiometric energy efficiency of the reaction amounts to 83.3% in case the low heating value of hydrogen (120 GJ/t) and methane (50 GJ/t) is considered (50 GJ/t/0.5  $\times$  120 GJ/t; Bernacchi et al. 2014a,b) and the process utilities are omitted. The “chemical Sabatier” is pursued as a heterogeneously catalyzed gas phase reaction. The catalyst is sensitive toward contaminations in the feed stream, such as hydrogen sulfide and siloxanes, which need to be removed. This defines a disadvantage versus the biological methanation, which is more robust with respect to contaminations in the feed stream (Leonzio 2016; Strevett et al. 1995). The selectivity is rather efficient. Partially the typical nickel hydrogenation catalyst has been replaced by a more expensive ruthenium catalyst which is less prone to decomposition (Burkart et al. 2019). The conversion of the reaction is incomplete and a recycling of the non-converted educts is required. The “Le Chatelier” principle favors a low temperature of the exothermic reaction and a high pressure which, however, would raise the EHS requirements and the investment for an industrial plant. On the other hand, kinetics favors high temperature. Accordingly, a compromise of the reaction parameters is needed and several combinations have been tried. The reaction is often pursued at a pressure of about 100 bar to support conversion to the right side of the equilibrium at temperatures between 200 and 500  $^\circ\text{C}$  (Rönsch et al. 2016; Götz et al. 2014). Especially, efficient heat removal needs to be considered in the choice of the most suited reactor. Usually, fixed-bed reactors are used, though also fluidized-bed, monolith, foam, micro-channel, membrane-based, and slurry reactors were evaluated. Most methanation plants apply a fixed-bed reactor (Rönsch et al. 2016; Ghaib et al. 2016). The mechanism of the reaction is not yet fully elucidated and might proceed via carbon monoxide or a direct hydrogenation. Catalyst development is focusing on decreasing the reaction temperature to increase conversion of the exothermic reaction and to extend the catalyst’s

lifetime. The initial chemisorption of carbon dioxide is depending on the catalyst surface. Several metal combinations for catalyst design are tested comprising rhodium, ruthenium, palladium, nickel, alumina-supported nickel, silica-supported nickel, zirconia, and ceria (Frontera et al. 2017). Hereby low catalyst cost enabled by high activity and low metal cost are crucial for process economy and especially the noble metal catalysts Ru, Rh, and Pd shall be avoided (Zhou et al. 2016). A prominent pilot plant is the Audi “e-gas” project which operated a 6 MW power-to-methane plant in 2013. The hydrogen feed is pressurized to a level of 10 bar before it is channeled into the reactor. Heat removal is facilitated with a salt bath reactor (Ghaib et al. 2016).

A broad industrial application of the chemical Sabatier is not yet possible given the much higher cost for producing methane – compared to the exploitation of natural gas reservoirs – and the limited availability of green hydrogen with low or zero carbon footprint. At minimum 2.75 t carbon dioxide is consumed for producing of one-ton methane (44 g/mol/16 g/mol), though about 4.5 tons carbon dioxide might be released given a hydrogen unit consumption rate of 0.5 t hydrogen per ton methane and a carbon footprint of about 9 t carbon dioxide per ton hydrogen (including Scope 3) if generated via conventional steam methane reforming technology (Boulamanti and Moya 2017).

#### 1.4.2 The Biochemical Sabatier

The fermentative conversion of carbon dioxide into methane or the “biochemical Sabatier” is operated at temperatures below 100 °C and obtains liquid water as by-product. Since the evaporation energy is not absorbed in the gasification, the released heat is higher than in the chemical process and needs to be removed by cooling:



(Thema et al. 2019)

The enthalpy of the reaction is estimated according to Hess’s law:

$$\begin{aligned} \Delta H_{\text{R}}^{\circ} &= \Sigma \Delta H_{\text{f P}}^{\circ} - \Sigma \Delta H_{\text{f E}}^{\circ} = (-74.8 \text{ KJ/mol} + 2x - 285.8 \text{ KJ/mol}) - 393.3 \text{ KJ/mol} \\ &= -253.1 \text{ KJ/mol given} \end{aligned}$$

$$\Delta H_{\text{f}}^{\circ} \text{CO}_2 (\text{g}) = -393.3 \text{ KJ/mol}$$

$$\Delta H_{\text{f}}^{\circ} \text{CH}_4 (\text{g}) = -74.8 \text{ KJ/mol and}$$

$$\Delta H_{\text{f}}^{\circ} \text{H}_2\text{O} (\text{l}) = -285.8 \text{ KJ/mol}$$

The Gibbs free energy of the reaction has been estimated and reveals that the reaction is in principle sufficiently exergonic to pursue a fermentative technology:



(Goyal et al. 2016; Thauer et al. 2008)

A more realistic value of  $\Delta G^{\circ} = -126.6 \text{ KJ/mol}$  was obtained with Aspen at ambient pressure and 338 K or 65 °C (Bernacchi et al. 2014a,b). This value should in principle be sufficient in case the biochemical system efficiently manages to channel the energy potential toward the formation of ATP. For the biochemical conversion, it is critical that the Gibbs free

**Table 1.1** Comparison of chemical and biological CO<sub>2</sub> methanation.

	Chemical methanation	Biological methanation
Reaction	CO <sub>2</sub> (g) + 4 H <sub>2</sub> (g) → CH <sub>4</sub> (g) + 2 H <sub>2</sub> O (g)	CO <sub>2</sub> (g) + 4 H <sub>2</sub> (g) → CH <sub>4</sub> (g) + 2 H <sub>2</sub> O (l)
Phase	Gas phase reaction/200 °C – 500 °C	Liquid phase reaction/<70 °C
Enthalpy	ΔH <sub>R</sub> <sup>°</sup> = –164.8 kJ/mol	ΔH <sub>R</sub> <sup>°</sup> = –253.1 kJ/mol
Pressure	About 100 bar	<10 bar
Catalyst	Ni-based/nobel metal	Biocatalyst (methanogenic bacteria)
Reactor	Fixed bed/fluidized bed	CSTR
Challenge	Efficient removal of heat/catalyst sensitivity	Low solubility of H <sub>2</sub> Low space time yield

energy is sufficiently negative to allow in parallel the generation of ATP for cellular maintenance in resting cells. In case the same feedstock shall be applied to raise the inoculum also sufficient energy for microbial growth is needed. The Gibbs free energy of the fermentation pathway needs to provide a phosphoryl group transfer potential for the formation of ATP of at least –31.8 KJ/mol plus a surplus to account for realistic energy efficiency in the biological system (Thauer et al. 1977).

The reaction is implemented at moderate temperatures <100 °C pending on the heat resistance of the biocatalyst and is pursued at low pressure. A slow kinetics and a potentially weak mass transfer in the reactor are regarded as disadvantages compared to the chemical process (Ghaib et al. 2016).

The chemical methanation and the biological methanation are two competing technological approaches to convert green power into methane as energy storage (Table 1.1).

## 1.5 Biochemical Pathway Design

The biochemical pathway for the reduction of carbon dioxide toward methane covers several steps, and the involved co-factors may deviate between various species for which the ability of biological methanation has been reported. With respect to metabolic engineering, it can be concluded that still the native biochemical pathway for methane generation is pursued. The biological methanation is carried out by methanogenic bacteria, which are a diverse group of Archaea microorganisms characterized by their ability to produce methane (Balch et al. 1979). They are found in anoxic habitats, are highly sensitive toward oxygen, and, accordingly, require specific anaerobic cultivation procedures. Pending on the feedstock hydrogenotrophic (hydrogen), acetoclastic (acetic acid) and methylotrophic (methanol) methanogenesis are distinguished. The process exemplified by the archaeobacterial model organism *Methanococcus maripaludis*, a strictly anaerobic, hydrogenotrophic methanogen, is reconstructed as follows (Goyal et al. 2016; Table 1.2):

Altogether eight electrons need to be transferred to the fully oxidized C-atom of methane. Carbon dioxide in the first step reacted with methanofuran (MFR) to provide formyl-THF as the first reduction product after having received two electrons from reduced ferredoxin (Figure 1.2).

**Table 1.2** Biochemical pathway for the generation of methane.

$\text{CO}_2 + \text{MFR} + \text{Fd}_{\text{red}} \rightarrow \text{Formyl-MFR} + \text{Fd}_{\text{ox}} + \text{H}_2\text{O}$	$\Delta G^{\circ\prime} = 0.0 \text{ KJ/mol}$ (Thauer et al. 2008)
$\text{Fd}_{\text{ox}} + \text{H}_2 + \text{PMF} \rightarrow \text{Fd}_{\text{red}}$	
$\text{Formyl-MFR} + \text{THMPT} \rightarrow \text{Formyl-THMPT} + \text{MFR}$	$\Delta G^{\circ\prime} = -5.0 \text{ KJ/mol}$ (Thauer et al. 2008)
$\text{Formyl-THMPT} \rightarrow \text{Methenyl-THMPT} + \text{H}_2\text{O}$	$\Delta G^{\circ\prime} = -5.0 \text{ KJ/mol}$ (Thauer et al. 2008)
$\text{Methenyl-THMPT} + \text{F420}_{\text{red}}\text{H}_2 \rightarrow \text{Methylene-THMPT} + \text{F420}_{\text{ox}}$	$\Delta G^{\circ\prime} = 6.0 \text{ KJ/mol}$ (Thauer et al. 2008)
$\text{Methylene-THMPT} + \text{F420}_{\text{red}}\text{H}_2 \rightarrow \text{Methyl-THMPT} + \text{F420}_{\text{ox}}$	$\Delta G^{\circ\prime} = -6.0 \text{ KJ/mol}$ (Thauer et al. 2008)
$2 \text{F420}_{\text{ox}} + 2 \text{H}_2 \rightarrow 2 \text{F420}_{\text{red}}\text{H}_2$	$\Delta G^{\circ\prime} = -11.0 \text{ KJ/mol}$ (Thauer et al. 2008)
$\text{Methyl-THMPT} + \text{CoM-SH} \rightarrow \text{Methyl-S-CoM} + \text{THMPT}$	$\Delta G^{\circ\prime} = -30.0 \text{ KJ/mol}$ (Thauer et al. 2008)
$\text{Methyl-S-CoM} + \text{HS-CoB} \rightarrow \text{CH}_4 + \text{CoM-S-S-CoB}$	$\Delta G^{\circ\prime} = -30.0 \text{ KJ/mol}$ (Thauer et al. 2008)
$\text{CoM-S-S-CoB} + \text{H}_2 \rightarrow \text{CoM-SH} + \text{CoB-SH}$	$\Delta G^{\circ\prime} = -39.0 \text{ KJ/mol}$ (Thauer et al. 2008)
<hr/>	
$\text{CO}_2 + 4 \text{H}_2 \rightarrow \text{CH}_4 + 2 \text{H}_2\text{O}$	$\Delta G^{\circ\prime} = -131.0 \text{ KJ/mol}$ (Thauer et al. 2008)

MFR, methanofuran; Fd, ferredoxin; THMPT, tetrahydrosarcinapterin; HS-CoB, coenzyme B; HS-CoM, coenzyme M. The standard free energy was calculated from equilibrium constants or from the standard free energies for formation at 25 °C with H<sub>2</sub>, CO<sub>2</sub>, and CH<sub>4</sub> in the gaseous state at 10<sup>5</sup> Pa, H<sub>2</sub>O in the liquid state, pH at 7.0 and all other compounds at 1 M activity.

Source: Adapted from Thauer et al. (2008).

This step is facilitated by the Fwd/Fmd enzyme, a tungsten-molybdenum containing formylmethanofuran dehydrogenase. The preceding reduction of ferredoxin may be facilitated via EchA or the Vhu/Hdr bifurcation complex. In the statement of the reaction, the pathway via the EchA enzyme is assumed which additionally uses a proton motive force (PMF) in order to provide the required reduction potential for the reduction of ferredoxin (−500 mV) which cannot be achieved with hydrogen (−414 mV) alone. Alternatively, the reduction of ferredoxin might be facilitated by the Vhu/Hdr bifurcation complex. It consumes 2 mol of hydrogen and additionally accomplishes the reduction of the disulfide bridge in CoM-S-S-CoB to regenerate the cofactors with each carrying a reduced sulfhydryl function. In the second step, the formyl group is transferred to THMPT (tetrahydromethanopterin) arranged by the formyltransferase to obtain formyl-THMPT. Formyl-THMPT is the subject of a dehydration facilitated by the methylene-THMPT cyclohydrolase (Mch) to obtain methenyl-THMPT. Afterward four electrons are transferred by two mol of F420<sub>red</sub> to obtain methylene-THMPT in the first step and Methyl-THMPT in the second step whereby the electron-providing cofactor is oxidized. The regeneration and reduction, respectively, of F420 are facilitated by the oxidation of hydrogen. The derived methyl function is handed over by a membrane-bound enzyme complex, namely, the methyltransferase (Mtr), to coenzyme M to obtain Methyl-S-CoM with activated thioester

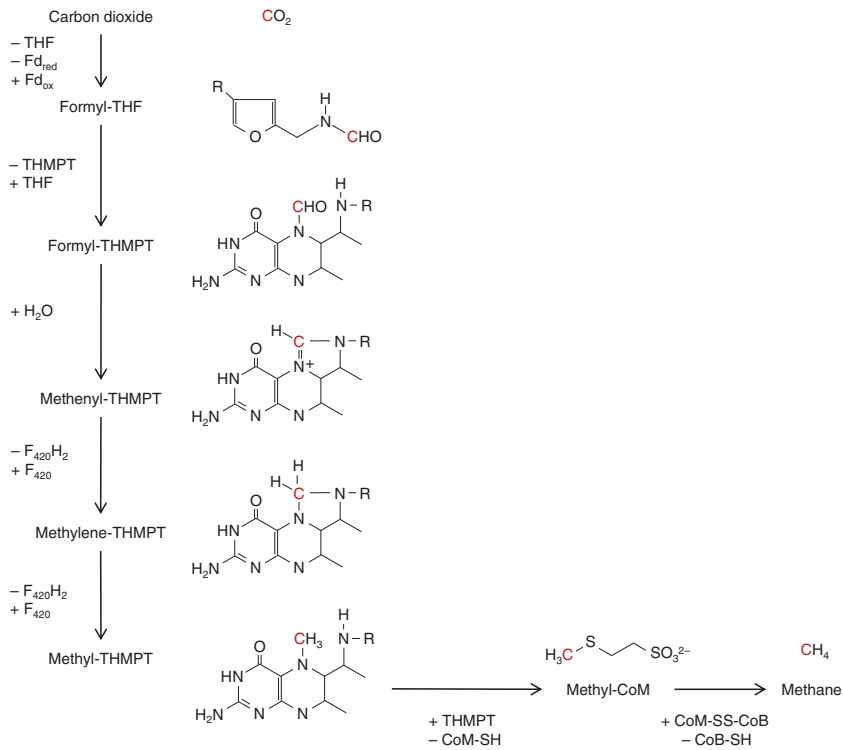


**Figure 1.2** Biochemical pathway for the conversion of carbon dioxide into methane (Sowers 2009). Source: Walter Koch.

in a highly exergonic reaction. This methyl transfer is coupled to the translocation of two sodium ions to generate a sodium gradient which drives an ATP synthase. Finally, methyl-S-CoM is subject to a reductive demethylation to obtain methane. The oxidized disulfide bridge between the co-factors CoM and CoB is recycled via a reduction with molecular hydrogen (Goyal et al. 2016).

The limited metabolic engineering tools for metabolic engineering of methanogenic bacteria had blocked the implementation of pathway improvement projects in the past. The recent progress with respect to the model organism *Methanothermobacter* – the microbe of the year 2021 – may change this and might allow the generation of other products than methane (Molitor et al. 2023).

## 1.6 Integration of Hydrogen Production and the Biochemical Methanation

### 1.6.1 Conversion of Carbon Dioxide into Methane with Integrated Production of Hydrogen

The fermentative reduction of carbon dioxide to methane as outlined above relies on the external supply of molecular hydrogen. Since the conversion of carbon dioxide into

**Table 1.3** Generation of methane coupled with the electrolysis of water.

$4 \text{ H}_2\text{O (l)} \rightarrow 4 \text{ H}_2 \text{ (g)} + 2 \text{ O}_2 \text{ (g)}$	$\Delta H_{\text{R}}^{\circ} = 285.8 \text{ KJ/mol H}_2\text{O}$
$\text{CO}_2 \text{ (g)} + 4 \text{ H}_2 \text{ (g)} \rightarrow \text{CH}_4 \text{ (g)} + 2 \text{ H}_2\text{O (l)}$	$\Delta H_{\text{R}}^{\circ} = -253.1 \text{ KJ/mol CH}_4$
$\text{CO}_2 \text{ (g)} + 2 \text{ H}_2\text{O (l)} \rightarrow \text{CH}_4 \text{ (g)} + 2 \text{ O}_2 \text{ (g)}$	$\Delta H_{\text{R}}^{\circ} = 890.1 \text{ KJ/mol CH}_4$ (Thema et al. 2019)

methane is from a sustainability point of view exclusively justified in case hydrogen is generated without significant emissions of carbon dioxide, water electrolysis driven by green power is needed unless rather infinite capacities for Carbon capture and storage (CCS) projects are granted. Thus, the external supply of hydrogen supposes an infrastructure for transportation and presumable storage which is circumvented in case the generation of hydrogen and the hydrogenation of carbon dioxide are integrated (Mayer et al. 2017). The integration of electrical green power to drive the water electrolysis with the conversion of carbon dioxide into methane avoids the generation, storage, and eventually the transportation of hydrogen. Since an infrastructure for the storage and transportation of hydrogen is usually not yet available – with the exemption of some chemical clusters with steam methane reformer (SMR) plants and adjacent hydrogenation plants – the technology integration might be an advantage for future application. The green power generated by wind turbines and photovoltaics could directly be used to obtain methane which would then be used or stored in local gas grids. The overall reaction is derived as the addition of the two single reactions shown below. The high endothermic character of the reaction is due to the high energy input for splitting water (Table 1.3):

The enthalpy of the reaction is confirmed by application of Hess's law:

$$\Delta H_{\text{R}}^{\circ} = \Sigma \Delta H_{\text{f}}^{\circ} \text{ P} - \Sigma \Delta H_{\text{f}}^{\circ} \text{ E} = -74.8 \text{ KJ/mol} - (-393.3 \text{ KJ/mol} + 2x - 285.8) = 890.1 \text{ KJ/mol}$$

$$\Sigma \Delta H_{\text{f}}^{\circ} \text{ CO}_2 \text{ (g)} = -393.3 \text{ KJ/mol},$$

$$\Sigma \Delta H_{\text{f}}^{\circ} \text{ CH}_4 \text{ (g)} = -748 \text{ KJ/mol and}$$

$$\Sigma \Delta H_{\text{f}}^{\circ} \text{ H}_2\text{O (l)} = -2858 \text{ KJ/mol}$$

In case the electrolysis of water is integrated with the fermentative hydrogenation of carbon dioxide, the field of microbial electrosynthesis (MES) is entered. MES is a developing technology to provide electrical power for fermentation systems providing electrons for the buildup of reducing equivalents, which can be used for the reduction of material feedstocks (Gong et al. 2020; Jafary et al. 2015). The common setup foresees to install an anode and a cathode in a two-chambered system with separated anode and cathode space. Once a sufficient potential is applied, water splitting proceeds at the anode which forms molecular oxygen, protons, and electrons. The potential at the cathode may be controlled with a potentiostat to ensure a sufficient potential for the generation of hydrogen through or to block a short-term high potential that might hurt the host or the biofilm, respectively. This measure is reasonable in R&D but might be impractical for a commercial application. The oxygen is not needed and is released into the reactor headspace. The protons diffuse into the cathode space via a proton-exchange membrane and receive electrons at the cathode for the generation of fermentative reduction equivalents. In order to save purchasing of

membranes, which likely need to be replaced in defined intervals, a membrane-less reactor has been proposed (Giddings et al. 2015). The vertical arrangement of both electrodes with the anode above the cathode in membrane-less reactor ensures that the formed and ascending oxygen does not interfere with the oxygen-sensitive host in the cathode space.

### 1.6.2 Mechanisms at the Cathode for the Uptake of Reduction Equivalents

The uptake of reduction equivalents by the biocatalyst may proceed via different mechanisms and three modes of interaction are distinguished (Enzmann et al. 2018; Mayer et al. 2019). In case a direct electron transfer (DET) is assumed, the organism would be in contact with the cathode via cytochromes, membrane-bound proteins, conductive filaments (so-called “nanowires”), or outer membrane extensions. The microbial host usually forms a biofilm on the cathode. A DET mechanism is assumed for the species *Geobacter sulfurreducens* and *Shewanella oneidensis*. The metabolic abilities of the microorganisms inhabiting the cathode surface are not yet fully understood. Transcriptome analysis of host community members isolated in the supernatant of the cathode or near the cathode surface revealed a distinct expression pattern of soluble hydrogenases, ferredoxins, formate dehydrogenases, and cytochromes which are likely involved in the metabolic management of the electron flow (Marshall et al. 2017; Perona-Vico et al. 2020).

A mediated electron transfer (MET) is assumed in case a redox-active component receives the electrons from the cathode and channels them to the fermentation host. The mediator might be added to the biochemical system or be induced and self-secreted by the host. *S. oneidensis* is known to secrete riboflavin as redox mediator. A MET is assumed for *Escherichia coli* mediated by neutral red; a cationic dye that is used as a histological stain due to its optical sensitivity to pH in the physiological range between pH 6–8. If neutral red is added to the medium, it is protonated with protons out of the cathode medium and receives electrons from the cathode. It diffuses into the inner membrane and transfers the electrons to menaquinone, which diffuses within the membrane to the active site of a terminal reductase or to the arcB enzyme which ultimately delivers the electrons to a terminal electron acceptor like fumarate (Harrington et al. 2015).

Additionally, an indirect electron transfer (IET) might proceed in which the electrons at the cathode are received by the protons generated at the anode and molecular hydrogen is abiotically synthesized without the involvement of the microbial host. The hydrogen would then be absorbed by the microorganism submerged in the cathode medium for the biochemical hydrogenation steps (Enzmann et al. 2018). In case an abiotic hydrogen generation is pursued, it is crucial to establish an efficient uptake of the molecular hydrogen in *statu nascendi* to avoid diffusion of the costly reduction agent into the reactor headspace. With respect to *Sporomusa ovata*, it could be shown that the biofilm at the cathode is highly effective in scavenging the evolving hydrogen (Giddings et al. 2015).

MES is pursued for different interests pending on the target molecule. It might be used to provide additional electrons in case the fermentation feedstock does not provide sufficient electrons for the target pathway, e.g. in the fermentative production of 1,3-propanediol based on glucose (Kracke and Krömer 2014). So far several molecules including acetic acid, butyric acid, isobutyric acid, isopropanol, butanol, and isobutanol could be produced via MES from carbon dioxide and electricity (Cheng et al. 2009; Ganigué et al. 2015; Nevin et al. 2011; Vassilev et al. 2018). MES might alternatively be tested in case a highly or

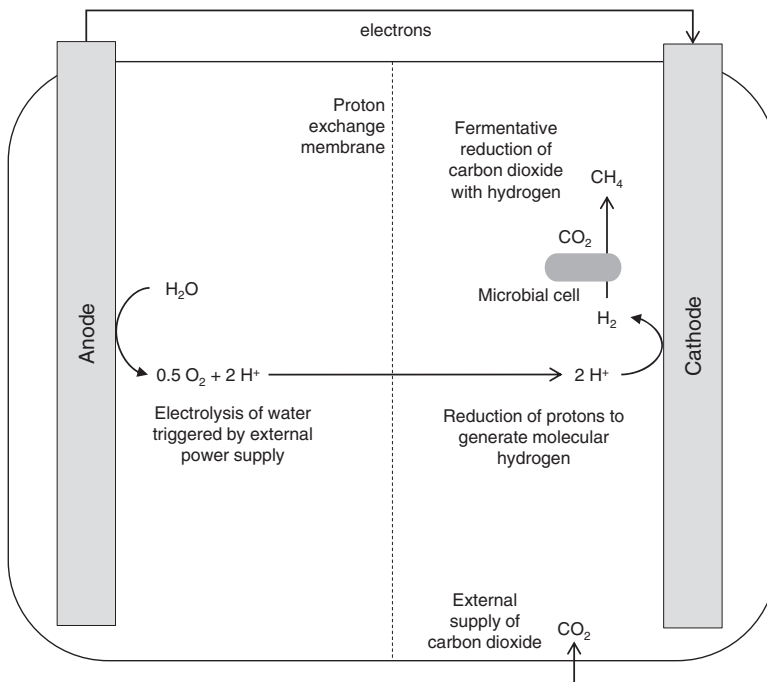


**Figure 1.3** Integrated bioelectrochemical system consisting of a water electrolysis combined with the fermentative reduction of carbon dioxide toward methane. Source: Adapted from Kracke et al. (2019).

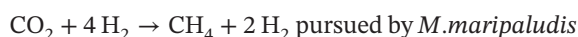
fully oxidized feedstock shall be reduced to obtain a biofuel. This approach is pursued for producing methane based on carbon dioxide, water, and electrical power.

### 1.6.3 R&D with Integrated Hydrogen Production and Biochemical Methanation and IET

Proof of concept based on experimental data for the combination of water electrolysis integrated with the fermentative reduction of carbon dioxide via IET has been shown (Kracke et al. 2019). The bio-electrochemical reactor consists of two chambers with a volume of 150 ml separated by a Nafion proton-exchange membrane with a surface area of 7.5 cm<sup>2</sup>. It avoids the diffusion of oxygen into the cathode chamber where the oxygen-sensitive hosts are cultivated (Figure 1.3).

In the first step, the formation of molecular hydrogen at the cathode was shown by applying either cobalt-phosphide (CoP), molybdenum-disulfide (MoS<sub>2</sub>), or nickel-molybdenum (NiMo) alloy as cathode materials. The commonly used and cheaper carbon-based cathode was ruled out since microbial electrosynthesis is pursued under specific conditions – neutral pH in the presence of media components for the biocatalyst – and instead, cathode materials including transition metals were evaluated, which are known to significantly increase the hydrogen evolution rate in MES. These cathodes were tested with respect to their biocompatibility for the generation of hydrogen. The cathode space was sparged with carbon dioxide at neutral pH in 0.03 M NaHCO<sub>3</sub>. Applying a constant current of 1 mA/cm<sup>2</sup>

and a potential of  $-1\text{ V}$  versus the standard hydrogen electrode (SHE), a maximum hydrogen production rate of  $48\ \mu\text{mol/h} \times \text{cm}^2$  observed for the NiMo cathode is achieved with a Coulomb efficiency of 98%. Coulomb efficiency was calculated by dividing the electrons recovered in the target molecule by the electrons supplied as current for a defined incubation time. In the next steps, the cathode efficiency was tested after microbial media were added to the electrolyte suitable for methanogenic and homoacetogenic bacteria. It could be observed that the Coulomb efficiency decreased in the homoacetogenic medium likely due to the unspecific reduction of organic media compounds. After separate analysis and confirmation of hydrogen formation, the cathode space was inoculated with either the homoacetogenic bacterium *S. ovata* or the methanogenic archaeon *M. maripaludis*. Both would use the generated hydrogen for producing either methane or acetic acid.



The MES would proceed via an IET and the evolved hydrogen is used by the hosts as electron source either to produce methane or acetic acid. It could be shown that an elevated hydrogen concentration could exclusively be found in close proximity to  $50\text{--}100\ \mu\text{m}$  of the cathode surface. The hydrogen concentration was  $0.2\text{--}0.6\ \mu\text{mol/l}$  in the medium containing the biocatalyst and around  $220\ \mu\text{mol/l}$  without the biocatalyst. This efficient hydrogen uptake is seen as an advantage since it avoids the development of a DET, which may restrict the repertoire of suitable hosts, and facilitates efficient production rates. With an electron supply rate of  $3.73 \times 10^{-2}\ \text{mmol/h}$ , a methane generation of  $9.16 \times 10^{-3}\ \text{mmol/h}$  (Coulomb efficiency 98.2%) and an acetic acid generation of  $4.7 \times 10^{-3}\ \text{mmol/h}$  (Coulomb efficiency 100.8%), respectively, could be observed (Kracke et al. 2019). The supply of electrons and the generation of methane and acetic acid (indicated as electron equivalents) were plotted against time (batch duration 50 hours). A proportional relation was shown as expected.

#### 1.6.4 Boundary Conditions for Potential Commercial Application

The commercial attractiveness of the integrated hydrogen production depends mainly on the overall energy efficiency of the microbial electro-fermentation. The benchmark for the integrated approach is the external supply of green hydrogen generated by water electrolysis (polymer exchange membrane; PEM), which has an energy usage of  $50\ \text{MWh/t H}_2$  (Tountas et al. 2021; Götz et al. 2016). In case the hydrogen yield in the fermentative conversion of carbon dioxide with hydrogen to methane (without microbial electrosynthesis) is assumed with 98% and the corresponding hydrogen unit consumption rate is  $0.51\ \text{t H}_2/\text{t CH}_4$ , the overall power consumption of the process would be  $25.5\ \text{MWh/t H}_2$  without including the power demand in the fermentation process itself, e.g. gas compression and downstream purification ( $50.0\ \text{MWh/t H}_2 \times 0.51\ \text{t H}_2/\text{t CH}_4$ ).

For comparison, the power consumption for the integrated hydrogen production and biochemical methanation can be estimated based on the available information keeping in mind that the mini setup of the experiments is not designed to accomplish a potential commercial efficiency. The estimation outlined below refers to the work of Prof. Spormann at Stanford University (Kracke et al. 2019). In one experiment, a hydrogen evolution rate of

$39 \mu\text{mol}/\text{cm}^2 \times \text{h}$  was achieved with a platinum cathode. The constant potential was  $-1.0 \text{ V}$  versus SHE. The cathode surface area is  $1 \text{ cm}^2$  and the current density is given with constant  $1 \text{ mA}/\text{cm}^2$  for all experiments. The intensity of current of the system can be derived with  $1 \text{ mA}$ . Thus, given that  $1 \text{ W} = 1 \text{ V} \times 1 \text{ A}$  and  $1 \text{ A} = 1 \text{ C}/\text{s}$ , it can be derived that 1 hour of incubation implies an electrical work of  $3.6 \text{ Wh}$ . In this  $1 \text{ h } 39 \mu\text{mol } [\text{H}]/\text{cm}^2$ , cathode area is generated translating into  $39 \mu\text{mol}$  hydrogen absolute generation within the system:

$3.6 \text{ Wh}$  corresponds to  $39 \mu\text{mol } [\text{H}]$ , derive

$3.6 \text{ Wh}$  corresponds to  $39 \mu\text{g } \text{H}_2$ , derive

$0.092 \text{ Wh}$  corresponds to  $1 \mu\text{g } \text{H}_2$ , derive

$92 \text{ MWh}$  corresponds to  $1 \text{ kg } \text{H}_2$

The cathode has absorbed  $3.6 \text{ C}$  in  $1 \text{ h}$ . The derived  $39 \mu\text{mol } [\text{H}]$  requires  $3.76 \text{ C}$  ( $96.485 \text{ C}/\text{mol}$ ) and the indicated Coulomb efficiency of  $99\%$  is plausible given a realistic measurement accuracy of the system. Accordingly, the derived power consumption in the experimental system is  $1840$ -fold higher than the consumption in the fully optimized stand-alone PEM water electrolysis. The huge gap indicates the ambitious development target of such a system to achieve commercial maturity. Especially, the intensity of current needs to be increased up to a range of  $100$ – $1000 \text{ mA}/\text{cm}^2$  (Kracke et al. 2021).

The high-power unit consumption rate is caused by several reasons. It is in the first instance not realistic to achieve a commercially interesting usage rate in the experimental setup. The whole system is designed to optimize the biochemical conversion of carbon dioxide. Anode and cathode space for the electrolysis of water is optimized with respect to the requirements of the biocatalyst (i.e.  $\text{pH } 7.0$ , media components) and not for electrochemical efficiency. The suitability of the integrated system for the methanogenic host *M. maripaludis* allows to use its specific ability for IET and thereby avoids the tedious development of a technology with DET. Specific cathode material is evaluated and the high experience in cathode material development for a conventional alkaline electrolysis (AE) or the PEM technology can likely not be exploited.

## 1.7 Process Development for the “Biochemical Sabatier” without Integrated Water Electrolysis

The feeding of a gas stream consisting of carbon dioxide and hydrogen and its circulation within the reactor defines a critical hurdle for facilitating an efficient productivity. Carbon dioxide has a reasonable solubility in water via the formation of bicarbonate, though hydrogen might display a limiting accessibility for the host and might negatively impact space-time yield. Solubility of hydrogen is increased with lowered temperature and raised pressure. Whereas the first option is limited given the temperature sensitivity of the biocatalyst the pressure can be raised to some extent although then also the methane pressure in the reactor headspace would be higher (Leonzio 2016). In a process simulation using Aspen, a theoretically optimized pressure of  $11 \text{ bar}$  could be identified at which about  $80\%$  of the total carbon dioxide feed is converted (Bernacchi et al. 2014a,b). The critical mass transfer

and the corresponding hydrogen consumption of the biocatalyst are enhanced with a high mass transfer coefficient  $K_L$ , an increased surface area between the gas bubbles and the outer host membrane, and the hydrogen concentration gradient in the liquid phase and the gas phase.

Several reactor types have been considered to address this challenge (Thema et al. 2019). In the continuously stirred tank reactor (CSTR), the microorganism is suspended in the liquid phase, and the feed gases are introduced at the bottom of the reactor. The stirrer would permanently be mixing the liquid and the gaseous phase and especially provide a high surface area via a reduction of the size of the gas bubbles. The heat of the exothermic reaction is removed with cooling equipment. The methane product stream including non-converted educts is captured at the reactor head and channeled into the downstream process section. Alternatively, a bubble column reactor (BCR) might be employed in which the pressurized gas stream of carbon dioxide and hydrogen ensures efficient mixing of both phases in the reactor. A stirrer would not be needed. The saved power demand is counterbalanced by the efforts to pressurize the feed gases. An interesting approach to address the difficult accessibility of hydrogen for the biocatalyst would be the trickle-bed reactor (TBR), which is packaged with small solid particles to facilitate a small diameter and, accordingly, a huge overall surface of the hydrogen and carbon dioxide gas bubbles which are fed into the reactor at the bottom. The biocatalyst might be immobilized on the surface of the solid particles or be suspended in the liquid phase containing the medium. The liquid phase is captured at the bottom of the reactor and pumped for recirculation to the head of the reactor. In this step, also the heat of the reaction would be removed (Thema et al. 2019). The published mass transfer coefficients  $k_L$  are for all three reactor types in the range of 0.3 up to  $4 \times 10^{-4}$  m/s. With respect to the range of the effective surface area  $a_{\text{eff}}$ , the CSTR and the BCR are subscribed with 100 up to  $1500 \text{ m}^{-1}$  higher values than the TBR with 60 up to  $640 \text{ m}^{-1}$  (Thema et al. 2019). The innovative concepts of a TBR or a BCR might provide a better solution for the biological methanation. However, the applied known reactor of the pilot plant of *Electrochaea* is a conventional CSTR with a height of 9 m and four impellers (Rusmanis et al. n.d.). It remains to be seen if this reactor concept turns out to be the superior solution for the fermentative generation of methane or if the alternative reactor concepts are finally chosen after additional development work has been done.

## 1.8 Commercial Application of Fermentative Methane Production

The biochemical conversion of carbon dioxide to methane with external supply of hydrogen is pursued by the companies *Electrochaea* ([www.electrochaea.com](http://www.electrochaea.com)) and *Krajete* ([www.krajete.com](http://www.krajete.com)). Their technology is not yet commercialized in high-volume plants, though a broader application is to be expected. The production of SNG, either via the chemical or the biochemical methanation, is still suffering from the high costs of green hydrogen. Whereas the cost of conventional natural gas amounts to 30 €/MWh in Europe, the cost of SNG derived via the methanation of carbon dioxide is estimated to 400 €/MWh (Vahrenholt 2023).

The performance of the *Electrochaea* technology is described in this section since detailed information of their pilot plant in Denmark is available (*Electrochaea* 2014;

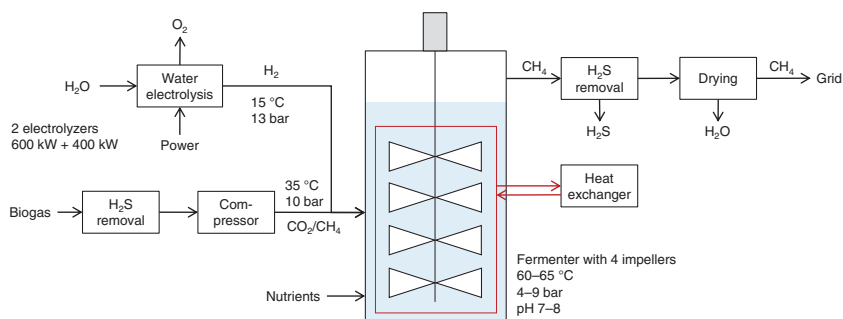


**Figure 1.4** Flow diagram for the conversion of carbon dioxide with hydrogen into methane according to Electrochaeta. Source: Walter Koch.

Rusmanis et al. n.d.). The technology has been demonstrated in a pilot scale in Denmark at the BIOFOS Avedøre wastewater treatment center and Electrochaeta is offering the technology to commercial partners. The first commercial plant shall be constructed in Denmark and a funding of 36 € m has been secured in 2022 (Krapp 2022). Electrochaeta applies a nongenetically modified archaea bacterium and combines water electrolysis with the fermentative production of methane. The feedstock is raw biogas, though also carbon dioxide might be used. The methane purity in the reactor headspace is reported higher than 97% and exceeds the critical threshold of 96% methane in compliance with local and national requirements of grid operators (Figure 1.4).

Accordingly, the methane can be injected into the gas grid as SNG. The technical ability to achieve a grid injection level gas quality is crucial for the commercial application of the technology and a major boundary condition for process design. Electrochaeta succeeded in meeting the 96% threshold by using a high mixing rate, elevated pressure, and a pure strain archaea culture (Rusmanis et al. n.d.).

The process displays a high on/off flexibility which might be useful in case renewable power is applied for producing hydrogen (<http://electrochaeta.com> 2021). Based on patents (Electrochaeta patent 2020), it may be assumed that the reaction is pursued at a temperature around 60–65 °C (Bernacchi et al. 2014a,2014b) and a pH of about 7.0. The dead biomass might be kept in the reactor together with the still-active cells because the nutritional components of the dead biomass are partially released and absorbed by the living cells. Although it is common sense that oxygen inhibits important enzymes in biological methanogenesis and hampers productivity, it is reported that microaerobic conditions and minor residues of H<sub>2</sub>S can be tolerated by some modified species. This would especially limit efforts for feedstock processing and purification. A culture of *Methanothermobacter thermoautotrophicus* with a biomass concentration of 10–12 g/l is reported in an Electrochaeta patent to display a productivity of 40 l CH<sub>4</sub>/l × d which is corresponding to a productivity of 1.2 g/l × h (Electrochaeta 2020). In case this level could be achieved in the pilot plant, it would be in the range of typical fermentation productivities up to 4 g/l × h. However, based on conference presentations, a conversion of even 800 l CH<sub>4</sub>/l × d is reported which is corresponding to an outstanding productivity of 24 g/l × h (Rusmanis et al. n.d.). This value is corresponding to the methane stream obtained in the reactor headspace, but it needs to be taken into consideration that raw biogas – which a methane content of 50%–60% (v/v) – has been applied as feedstock, and the synthetic productivity in the reactor is likely in the range of

about 12 g/l × h. The reactor operates at a temperature of 60–65 °C and a pressure of 4–9 bar (Rusmanis et al. n.d.). The pressure displays a gradient in the reactor. Since the reactor has a height of 8 m the broth pressure at the bottom of the reactor is about 1 bar higher than below the headspace of the reactor.

Less details are published on the status and the performance of the methanation technology executed by Krajete. Krajete also applies a CSTR, which is fed with hydrogen and carbon dioxide at the bottom. The methanogenic host tolerates some contaminations in the feed gas. The gas bubbles are dispersed by the stirrer, and a uniform distribution within the reactor is facilitated. Methane is captured at the headspace of the reactor. The process does display a high on/off flexibility and allows restart after 500 hours of interruption (Krajete homepage 2021).

## References

- Adnan, A.I., Ong, M.Y., Nomanbhay, S. et al. (2019). Technologies for upgrading biogas to biomethane: a review. *Bioengineering* 6: 92. <https://doi.org/10.3390/bioengineering6040092>.
- Arpe, H.-J. (2007). *Industrielle Organische Chemie. Bedeutende Vor- und Zwischenprodukte*. Wiley.
- Balch, W.E., Fox, G.E., Magrum, L.J. et al. (1979). Methanogens: reevaluation of a unique biological group. *Microbiological Reviews* 43: 260–296.
- Bernacchi, S., Weissgram, M., Wukovits, W., and Herwig, C. (2014a). Process efficiency simulation for key process parameters in biological methanogenesis. *AIMS Bioengineering* 1 (1): 53–71. <https://doi.org/10.3934/bioeng.2014.1.53>.
- Bernacchi, S., Rittmann, S., Seifert, A.H. et al. (2014b). Experimental methods for screening parameters influencing the growth to product yield ( $Y_{[x/CH_4]}$ ) of a biological methane production (BMP) process performed with *Methanothermobacter marburgensis*. *AIMS Bioengineering* 1 (2): 72–87. <https://doi.org/10.3934/bioeng.2014.2.72>.
- Boulamanti, A. and Moya, J.A. (2017). Energy efficiency and GHG emissions: prospective scenarios for the Chemical and Petrochemical Industry. JRC science for policy report, European Union, p. 17.
- Burkart, M.D., Hazari, N., Tway, C.L., and Zeitler, E.L. (2019). Opportunities and challenges for catalysis in carbon dioxide utilization. *ACS Catalysis* 9: 7937–7956. <https://doi.org/10.1021/acscatal.9b02113>.
- Capital (2019). LNG. Edition 4e, pp. 18–20. [www.capital.de](http://www.capital.de).
- Centi, G., Perathoner, S., Salladini, A., and Iaquaniello, G. (2020). Economics of CO<sub>2</sub> utilization: a critical analysis. *Frontiers in Energy Research* 8: <https://doi.org/10.3389/fenrg.2020.567986>.
- Cheng, S., Xing, D., Call, D.F., and Logan, B.E. (2009). Direct biological conversion of electrical current into methane by electromethanogenesis. *Environmental Science and Technology* 43: 3953–3958.
- Electrochaea (2014). Power-to-gas via biological catalysis (P2G-Biocat). Final report. [https://energiforskning.dk/sites/energiforskning.dk/files/slutrappporter/12164\\_final\\_report\\_p2g\\_biocat.pdf](https://energiforskning.dk/sites/energiforskning.dk/files/slutrappporter/12164_final_report_p2g_biocat.pdf).
- Electrochaea homepage (2021). [www.electrochaea.com](http://www.electrochaea.com) (accessed 14 November 2021).
- Electrochaea patent (2020). Method to use industrial CO<sub>2</sub> containing gas for the production of a methane enriched gas composition. 7.5.2020, WO 2020/089181 A1.

- Enzmann, F., Mayer, F., Rother, M., and Holtmann, D. (2018). Methanogens: biochemical background and biotechnological applications. *AMB Express* 8: 1. <https://doi.org/10.1186/s13568-017-0531-x>.
- Ewald, S., Koschany, F., Schlereth, D. et al. (2015). Power-to-gas. *Chemie in unserer Zeit* 49: 270–278. <https://doi.org/10.1002/ciuz.201500715>.
- Focus (2021). Faktenreport: Erdgas, primary data from Statistisches Bundesamt, Statista and DIW, p. 59.
- Frontera, P., Macaria, A., Ferraro, M., and Antonucci, P. (2017). Supported catalysts for CO<sub>2</sub> methanation: review. *Catalysts* 7: 59. <https://doi.org/10.3390/catal7020059>.
- Gan, Y., El-Houjeiri, H.M., Badahdah, A. et al. (2020). Carbon footprint of global natural gas supplies in China. *Nature Communications* 11: 824. <https://doi.org/10.1038/s41467-020-14606-4>.
- Ganigué, R., Puig, S., Batle-Vilanova, P. et al. (2015). Microbial electrosynthesis of butyrate from carbon dioxide. *Chemical Communications* 51: 3235–3238.
- Ghaib, K., Nitz, K., and Ben-Fares, F.-Z. (2016). Chemical methanation of CO<sub>2</sub>: a review. *Chemical Bioengineering Review* 3 (6): 266–275.
- Giddings, C.G.S., Nevin, K.P., Woodward, T. et al. (2015). Simplifying microbial electrosynthesis reactor design. *Frontiers in Microbiology* 6: 468. <https://doi.org/10.3389/fmicb.2015.00468>.
- Goeppert, A., Czaun, M., Jones, J.-M. et al. (2014). Recycling of carbon dioxide to methanol and derived products – closing the loop. *The Royal Society of Chemical*. <https://doi.org/10.1039/c4cs00122b>.
- Gong, Z., Yu, H., Zhang, J. et al. (2020). Microbial electro-fermentation for synthesis of chemicals and biofuels driven by bi-directional extracellular electron transfer. *Synthetic and Systems Biotechnology* 5: 304–313. <https://doi.org/10.1016/j.synbio.2020.08.004>.
- Götz, M., McDaniel Koch, A., and Graf, F. (2014). State of the art and perspectives of CO<sub>2</sub> methanation process concepts for power-to-gas application. Conference paper. [https://www.researchgate.net/publication/273139805\\_State\\_of\\_the\\_Art\\_and\\_Perspectives\\_of\\_CO2\\_Methanation\\_Process\\_Concepts\\_for\\_Power-to-Gas\\_Applications](https://www.researchgate.net/publication/273139805_State_of_the_Art_and_Perspectives_of_CO2_Methanation_Process_Concepts_for_Power-to-Gas_Applications).
- Götz, M., Lefebvre, J., Mörs, F. et al. (2016). Renewable power-to-gas: a technological and economic review. *Renewable Energy* 85: 1371–1390. <https://doi.org/10.1016/j.renene.2015.07.066>.
- Goyal, N., Zhou, Z., and Karimi, I.A. (2016). Metabolic processes of *Methanococcus maripaludis* and potential applications. *Microbial Cell Factories* 15: 107. <https://doi.org/10.1186/s12934-016-0500-0>.
- Güssgen, F., Tutt, C., and Wettach, S. (2021). Moskaus monopoly. *Wirtschaftswoche* 24 (9): 46–49.
- Handelsblatt (2022). Im Notfall Staatshilfe. p. 33.
- Harrington, T.D., Tran, V.N., Mohamed, A. et al. (2015). The mechanism of neutral red-mediated microbial electrosynthesis in *Escherichia coli*: menaquinone reduction. *Bioresource Technology* 689–695. <https://doi.org/10.1016/j.biortech.2015.06.037>.
- House, K.Z., Baclig, A.C., Ranjan, M. et al. (2011). Economic and energetic analysis of capturing CO<sub>2</sub> from ambient air. *PNAS* 108 (51): 20428–20433. <https://doi.org/10.1073/pnas.1012253108>.
- Jafary, T., Daud, W.R.W., Ghasemi, M. et al. (2015). Biocathode in microbial electrolysis cell: present status and future prospects. *Renewable and Sustainable Energy Reviews* 47: 23–33. <https://doi.org/10.1016/j.rser.2015.03.003>.

- Kracke, F. and Krömer, J.O. (2014). Identifying target processes for microbial electrosynthesis by elementary mode analysis. *BMC Bioinformatics* 15: 410. <https://doi.org/10.1186/s12859-014-0410-2>.
- Kracke, F., Wong, A.B., Maegaard, K. et al. (2019). Robust and biocompatible catalysts for efficient hydrogen-driven microbial electrosynthesis. *Communications Chemistry*. <https://doi.org/10.1038/s42004-019-0145-0>.
- Kracke, F., Deutzmann, J.S., Jayathilake, B.S. et al. (2021). Efficient hydrogen delivery for microbial electrosynthesis via 3D-printed cathodes. *Frontiers in Microbiology* 12: <https://doi.org/10.3389/fmicb.2021.696473>.
- Krajete homepage (2021). [www.krajete.com](http://www.krajete.com) (accessed 14 November 2021).
- Krapp, C. (2022). Electrochaeta 36 Millionen Euro für power-to-gas. *Handelsblatt* 7 (1): 19.
- Leonzio, G. (2016). Process analysis of biological Sabatier reaction for bio-methane production. *Chemical Engineering Journal* 290: 490–498. <https://doi.org/10.1016/j.cej.2016.01.068>.
- Marshall, C.W., Ross, D.E., Handley, K.M. et al. (2017). Metabolic engineering and modeling microbial electrosynthesis. *Scientific Reports* 7: 8391. <https://doi.org/10.1038/s41598-017-08877-z>.
- Mayer, F., Enzmann, F., Lopez, A.M., and Holtmann, F. (2017). Methanogene in der Elektrobiotechnologie. Die mikrobielle Elektrosynthese von Methan. *BIOspektrum* 4 (17): 471–473. <https://doi.org/10.1007/s12268-017-0825-1>.
- Mayer, F., Enzmann, F., Lopez, A.M., and Holtmann, D. (2019). Performance of different methanogenic species for the microbial electrosynthesis of methane from carbon dioxide. *Bioresource Technology*, <https://doi.org/10.1016/j.biortech.2019.121706>.
- Molitor, B., Casini, I., Fink, C. et al. (2023). Power-to-gas: neuer Rückenwind für ein altes Modellsystem. *Biospektrum* 1 (23): 94–96. <https://doi.org/10.1007/s12268-023-1880-4>.
- Nevin, K.P., Hensley, S.A., Franks, A.E. et al. (2011). Electrosynthesis of organic compounds from carbon dioxide is catalyzed by a diversity of acetogenic microorganisms. *Applied and Environmental Microbiology* 77 (9): 2882–2886. <https://doi.org/10.1128/AEM.02642-10>.
- OCI (2021). Q3 2021 results presentation. p. 17. <https://www.oci.nl/investor-centre/results-and-presentations> (accessed 23 December 2021).
- Ozkan, M., Nayak, S.P., Ruiz, A.D., and Jiang, W. (2022). Current status and pillars of direct air capture technologies. *iScience* 25 (103): 990.
- Perona-Vico, E., Feliu-Paradedá, L., Puig, S., and Bañeras, L. (2020). Bacteria coated cathodes as an in-situ hydrogen evolving platform for microbial electrosynthesis. *Scientific Reports* 10: 19852. <https://doi.org/10.1038/s41598-020-76694-y>.
- Rivard, E., Trudeau, M., and Zaghbi, K. (2019). Hydrogen storage for mobility. *Materials* 12: <https://doi.org/10.3390/ma.12.121.973>.
- Rönsch, S., Schneider, J., Matthischke, S. et al. (2016). Review on methanation. *Fuel* 166: 276–296. <https://doi.org/10.1016/j.fuel.2015.10.111>.
- Rusmanis, D., O’Shea, R., Wall, D.M., and Murphy, J.D. Biological hydrogen methanation systems – an overview of design and efficiency. *Bioengineered* 10 (1): 604–634. <https://doi.org/10.1080/21655979.2019.1684607>.
- Sowers, K.R. (2009). Methanogenesis. In: *Encyclopedia of Microbiology*, 3e (ed. M. Schaechter), 265–286. eBook ISBN 9780123739445.
- Spurgeon, J.M. and Kumar, B. (2018). A comparative technoeconomic analysis of pathways for commercial electrochemical CO<sub>2</sub> reduction to liquid products. *Energy & Environmental Science* 11: 1536–1551.

- Strevett, K.A., Vieth, R.F., and Grasso, D. (1995). Chemo-autotrophic biogas purification for methane enrichment-mechanism and kinetics. *Chemical Engineering Journal and the Biochemical Engineering Journal* 58 (1): 71–79.
- Thauer, R.K., Jungermann, K., and Decker, K. (1977). Energy conservation in chemotrophic anaerobic bacteria. *Bacterial Reviews* 41: 100–180. <https://doi.org/10.1128/MMBR.41.1.100-180.1977>.
- Thauer, R.K., Kaster, A.-K., Seedorf, H. et al. (2008). Methanogenic archaea: ecologically relevant differences in energy conservation. *Nature Reviews Microbiology* 6: 579–591.
- Thema, M., Weidlich, T., Hörl, M. et al. (2019). Biological CO<sub>2</sub> methanation: an approach to standardization. *Energies* 12: 1670.
- Thinkstep. (2017). GHG intensity of natural gas transport. [https://www.globalnghub.com/wp-content/uploads/attach\\_380.pdf](https://www.globalnghub.com/wp-content/uploads/attach_380.pdf).
- Tountas, A.A., Ozin, G.A., and Sain, M.M. (2021). Solar methanol energy storage. *Nature Catalysis* 4: 934–942. <https://doi.org/10.1038/s41929-021-00696-w>.
- Vahrenholt, F. (2023). *Die grosse Energiekrise und wie wir sie bewältigen*, 92. München: Langen Müller Verlag.
- Vassilev, I., Geißelmann, G., Schwechheimer, S.K. et al. (2018). Anodic electro-fermentation: anaerobic production of L-lysine by recombinant *Corynebacterium glutamicum*. *Biotechnology and Bioengineering* 115: 1499–1508. <https://doi.org/10.1002/bit.26562>.
- Zhou, R., Rui, N., Fan, Z., and Liu, C. (2016). Effect of the structure of Ni/TiO<sub>2</sub> catalyst on CO<sub>2</sub> methanation. *International Journal of Hydrogen Energy* 41: 22017–22025. <https://doi.org/10.1016/j.ijhydene.2016.08.093>.